Mon. Not. R. Astron. Soc. **325,** 636–648 (2001)

Stellar populations in the nuclear regions of nearby radio galaxies

Itziar Aretxaga,[1] Elena Terlevich,[1★†] Roberto J. Terlevich,[2‡] Garret Cotter[3] and Ángeles I. Díaz[4]

[1]*Instituto Nacional de Astrofísica, Óptica y Electrónica, Apdo. Postal 25 y 216, 72000 Puebla, Pue, Mexico*
[2]*Institute of Astronomy, Madingley Road, Cambridge CB3 0HA*
[3]*Cavendish Laboratory, Univ. of Cambridge, Madingley Road, Cambridge CB3 0HE*
[4]*Dept. Física Teórica C-XI, Univ. Autómoma de Madrid, Cantoblanco, Madrid, Spain*

Accepted 2001 February 25. Received 2001 February 5; in original form 2000 May 15

ABSTRACT

We present optical spectra of the nuclei of seven luminous ($P_{178\,\mathrm{MHz}} \gtrsim 10^{25}\,\mathrm{W\,Hz^{-1}\,Sr^{-1}}$) nearby ($z < 0.08$) radio galaxies, which mostly correspond to the FR II class. In two cases, Hydra A and 3C 285, the Balmer and λ4000-Å break indices constrain the spectral types and luminosity classes of the stars involved, revealing that the blue spectra are dominated by blue supergiant and/or giant stars. The ages derived for the last burst of star formation in Hydra A are between 7 and 40 Myr, and in 3C 285 about 10 Myr. The rest of the narrow-line radio galaxies (four) have a λ4000-Å break and metallic indices consistent with those of elliptical galaxies. The only broad-line radio galaxy in our sample, 3C 382, has a strong featureless blue continuum and broad emission lines that dilute the underlying blue stellar spectra. We are able to detect the Ca II triplet in absorption in the seven objects, with good quality data for only four of them. The strengths of the absorptions are similar to those found in normal elliptical galaxies, but these values are consistent both with stellar populations of roughly similar ages (as derived from the Balmer absorption and break strengths) and with mixed young+old populations.

Key words: galaxies: active – galaxies: starburst – galaxies: stellar content.

1 INTRODUCTION

In recent years new evidence has been gathered that indicates that *star formation plays an important role in Active Galactic Nuclei* (AGN).

(1) The presence of strong Ca II $\lambda\lambda$8494, 8542, 8662 Å triplet (CaT) absorptions in a large sample of Seyfert 2 nuclei has provided direct evidence for a population of red supergiant stars that dominates the near-IR light (Terlevich, Díaz & Terlevich 1990). The values found in Seyfert 1 nuclei are also consistent with this idea if the dilution produced by a nuclear non-stellar source is taken into account (Terlevich, Díaz & Terlevich 1990; Jiménez-Benito et al. 2000). The high mass-to-light ratios $L(1.6\,\mu\mathrm{m})/M$ inferred in Seyfert 2 nuclei also indicate that red supergiants dominate the nuclear light (Oliva et al. 1995), but a similar conclusion does not hold for Seyfert 1 nuclei.

(2) The absence of broad emission lines in the direct optical spectra of Seyfert 2 nuclei, which show broad lines in polarized light, can be understood only if there is an additional central source of continuum, most probably blue stars (Cid Fernandes & Terlevich 1995; Heckman et al. 1995). This conclusion is further supported by the detection of polarization levels which are lower in the continuum than in the broad lines (Miller & Goodrich 1990; Tran, Miller & Kay 1992).

(3) *Hubble Space Telescope* imaging of the Seyfert Mrk 447 reveals that the central UV light arises in a *resolved* region of a few hundred pc, in which prominent CaT absorption and broad He II λ4686-Å emission lines reveal the red supergiant and Wolf–Rayet stars of a powerful starburst. The stars dominate the UV to near-IR light directly received from the nucleus (Heckman et al. 1997). At least 50 per cent of the light emitted by the nucleus is stellar, as a conservative estimate. Mrk 447 is not a rare case: a large sample of nearby bright Seyfert 2s and low-ionization nuclear emission regions (LINERs) show similar resolved starburst nuclei of 80 to a few hundred pc in size (Colina et al. 1997; González-Delgado et al. 1998; Maoz et al. 1995, 1998), with some of the Seyfert 2s containing dominant Wolf–Rayet populations (Kunth & Contini 1999; Cid Fernandes et al. 1999).

A starburst–AGN connection has been proposed in at least three scenarios: starbursts giving birth to massive black holes (e.g. Scoville & Norman 1988); black holes being fed by surrounding

★E-mail: et@ast.cam.ac.uk (ET)
†Visiting Fellow at Institute of Astronomy, Cambridge.
‡Visiting Professor at Instituto Nacional Astrofísica, Óptica Electrónica, Mexico.

stellar clusters (e.g. Perry & Dyson 1985; Peterson 1992); and also pure starbursts without black holes (e.g. Terlevich & Melnick 1985; Terlevich et al. 1992). The evidence for starbursts in Seyfert nuclei strongly supports some kind of connection. However, it is yet to be demonstrated that starbursts play a key role in *all* kinds of AGN.

One of the most stringent tests *to assess if all AGN have associated enhanced nuclear star formation* is the case of lobe-dominated radio sources, the host galaxies of which have relatively red colours when compared to other AGN varieties. In this paper we address the stellar content associated with the active nuclei of a sample of Fanaroff–Riley (FR) II radio galaxies, the most luminous class of radio galaxies (Fanaroff & Riley 1974), which possess the most powerful central engines and radio jets (Rawlings & Saunders 1991). The presence of extended collimated radio jets, which fuel the extended radio structure over $\gtrsim 10^8$ yr, strongly suggests the existence of a supermassive accreting black hole in the nuclei of these radio galaxies. This test addresses the question of whether AGN that involve conspicuous black holes and accretion processes also contain enhanced star formation.

In Section 2 we introduce the sample and detail the data acquisition and reduction processes. In Section 3 we provide continuum and line measurements of the most prominent features of the optical spectra of the radio galaxies. In Section 4 we discuss the main stellar populations responsible for the absorption and continuum spectra. In Section 5 we offer notes on individual objects. A sumary of the main conclusions from this work is presented in Section 6.

2 DATA ACQUISITION AND REDUCTION

Our sample of radio galaxies was extracted from the 3CRR catalogue (Laing, Riley & Longair 1983) with the only selection criteria being edge-brightened morphology, which defines the FR II class of radio galaxies (Fanaroff & Riley 1974), and redshift $z < 0.08$. This last condition was imposed in order to be able to observe the redshifted CaT at wavelengths shorter than λ9300 Å, where the atmospheric bands are prominent. Six out of a complete sample of ten FR II radio galaxies that fulfill these requirements were randomly chosen. In addition to this sub-sample of FR IIs, we observed the unusually luminous FR I radio galaxy Hydra A (3C 218). This has a radio luminosity of $P_{178\,\mathrm{MHz}} = 2.2 \times 10^{26}\,\mathrm{W\,Hz^{-1}\,Sr^{-1}}$, which is an order of magnitude above the typical FR I/FR II dividing luminosity.

Spectroscopic observations of a total of seven radio galaxies, one normal elliptical galaxy to serve as reference and five K III stars to serve as velocity calibrators were performed using the double-arm spectrograph ISIS mounted in the Cassegrain Focus of the 4.2-m William Herschel Telescope in La Palma during two observing runs, in 1997 November 7–8 and 1998 February 19–20. The first run was photometric but the second was not, being partially cloudy on the 20th. The seeing, as measured from the spatial dimension of spectrophotometric stars, was between 0.7 and 0.8 arcsec throughout the nights.

A slit width of 1.2 arcsec centred on the nucleus of galaxies and stars was used. We oriented the slit along the radio axis for all radio galaxies, except for Hydra A, for which the orientation was perpendicular to the radio axis.

An R300B grating centred at λ4500 Å with a 2148x4200 pixel EEV CCD and an R316R grating centred at λ8800 Å with a 1024 × 1024 pixel TEK CCD were used in the 1998 run. The projected area on these chips is 0.2 arcsec pixel^{-1} and 0.36 arcsec pixel^{-1}, respectively. This configuration provides the spectral resolution necessary to resolve the Mg b and CaT features and, at the same time, offers a wide spectral span: λ3350–6000 Å at 5.1-Å resolution in the blue and λ7900–9400 Å at 3.5-Å resolution in the red. In the 1997 run, in which we assessed the viability of the project, we used the R600B and R600R gratings instead. This setup covers the λ3810–5420 Å and λ8510–9320 Å range in the blue and red arm, at 2.6- and 1.7-Å resolution respectively. Just one radio galaxy (DA 240) was observed with this alternative setup. The dichroics 5700 and 6100 were used in 1997 November and 1998 February, and in both runs we used a filter to avoid second-order contamination in the spectra.

We obtained flux standards (HZ 44 and G191 − B2B) for the four nights and gratings, except in 1998 February 20, when we were unable to acquire the red spectrum of the corresponding standard because of a technical failure. One calibration lamp CuAr+CuNe exposure per spectral region and telescope position was also obtained for all objects.

The total integration times for the radio galaxies (from 1–3 hr) were split into time intervals of about 1200 or 1800 s in order to diminish the effect of cosmic rays on individual frames and to allow us to take lamp flat-fields with the red arm of the spectrograph between science exposures. The TEK CCD has a variable fringing pattern at the wavelengths of interest, such that the variations are correlated with the position at which the telescope is pointing. Since flat-fielding is crucial for the reddest wavelengths, where the sky lines are most prominent, after every exposure of 20–30 min we acquired a flat-field in the same position of the telescope as the one for which the galaxies were being observed. We followed this procedure with all galaxies except DA 240. The same procedure was also used in the case of the elliptical galaxy, splitting its total integration time in two.

Table 1 summarizes the journal of observations, where column 1 gives the name of the object; column 2 the radio power at 178 MHz; column 3 the redshift; column 4 the integrated V magnitude of the galaxy; column 5 identifies whether the object is a radio galaxy (RG), a normal elliptical (E) or a star (S); column 6 gives the date of the beginning of the night in which the observations were carried out; column 7 the position angle (PA) of the slit; column 8 the total exposure time; column 9 the grating used; and column 10 the corresponding linear size to 1 arcsec at the redshift of the galaxies (for $H_0 = 50\,\mathrm{km\,s^{-1}\,Mpc^{-1}}$). The data for the radio galaxies were extracted from the 3C Atlas (Leahy, Bridle & Strom 1996, `http://www.jb.man.ac.uk/atlas/`) and for the host galaxy of Hydra A from the 3CR Catalogue (de Vaucouleurs et al. 1991).

The data were reduced using the IRAF software package. The frames were first bias subtracted and then flat-field corrected. In the case of the red-arm spectra, the different flats obtained for a single object were combined when no significant differences were detected between them. However, in several cases the fringing pattern shifted positions, which accounted for differences of up to 20 per cent. In these cases we corrected each science frame with the flat-field acquired immediately before and/or afterwards. Close inspection of the faintest levels of the flat-fielded frames showed that the fringing had been successfully eliminated. Wavelength and flux calibration were then performed, and the sky was subtracted by using the outermost parts of the slit.

The atmospheric bands, mainly water absorption at λ8920–9400 Å, affect the redshifted CaT region of several radio galaxies. The bands have been extracted using a template constructed from the stellar spectra obtained each night. The

Table 1. Journal of spectroscopic observations.

object	$P_{178\,\mathrm{MHz}}$ $\times 10^{25}\,\mathrm{W\,Hz^{-1}\,Sr^{-1}}$	z	V mag	type	date	PA ^{o}	exp. s	grating	l(1 arcsec) pc
3C 98	1.5	0.0306	15.9	RG	1998 Feb 19	221	8290	R300B	422
							8304	R316R	
3C 192	2.6	0.0598	16.1	RG	1998 Feb 19	133	7200	R300B	786
							7200	R316R	
3C 218 (Hydra A)	22.0	0.0533	12.6	RG	1998 Feb 20	113	10800	R300B	708
							10800	R316R	
3C 285	2.5	0.0794	15.9	RG	1998 Feb 20	66	10800	R300B	1010
							7200	R316R	
3C 382	2.2	0.0578	15.4	RG	1998 Feb 19	47	6200	R300B	762
							6200	R316R	
4C 73.08	1.6	0.0581	16.0	RG	1998 Feb 19	68	7200	R300B	765
							7200	R316R	
DA 240	0.9	0.0350	15.1	RG	1997 Nov 7	61	3600	R600B	479
							3900	R600R	
NGC 4374	–	0.0034	10.1	E	1998 Feb 19	135	1000	R300B	
							1000	R316R	49
G191-B2B	–	–		S	1997 Nov 7	–	300	R600B	
							300	R600R	
					1997 Nov 8		300	R600B	
							300	R600R	
HR 1908	–	–		S	1998 Feb 20	–	2	R300B	
							3	R316R	
HR 4575	–	–		S	1998 Feb 19	–	1	R300B	
							1	R316R	
HR 4672	–	–		S	1998 Feb 19	–	1	R300B	
							1	R316R	
HR 5826	–	–		S	1998 Feb 19	–	1	R300B	
							1	R316R	
HR 8150	–	–		S	1997 Nov 8	–	1	R600B	
							1	R600R	
HZ 44	–	–		S	1998 Feb 19	–	60	R300B	
							180	R316R	
					1998 Feb 20		60	R300B	

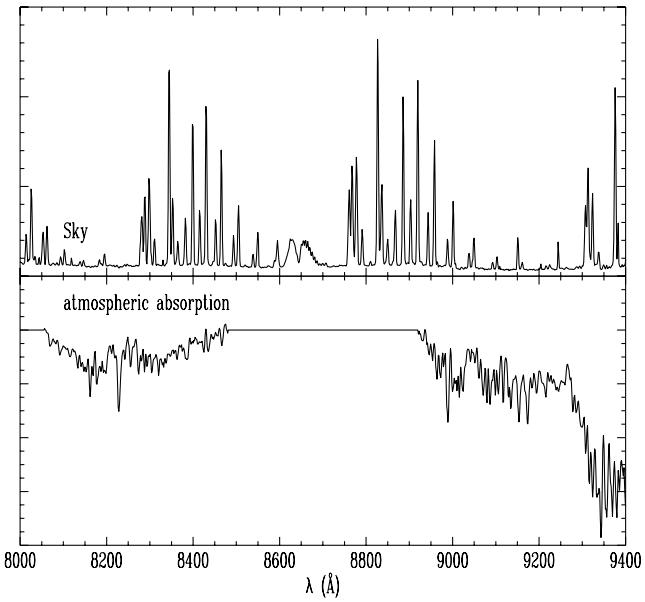

Figure 1. Sky line spectrum and atmospheric absorption template used to reduce the data.

template was built averaging the normalized flux of spectrophotometric and velocity standard stars, once the stellar absorption lines had been removed. The atmospheric bands were eliminated from the spectra of the galaxies dividing by the flux-scaled template. This reduces the signal-to-noise ratio (S/N) of the region under consideration, especially since the bands are variable in time and one of our observing nights was partially cloudy. However, the technique allows the detection of the stellar atmospheric features. The CaT of the elliptical galaxy is not affected by atmospheric absorption.

Fig. 1 shows the line spectrum of the sky and, as an example, the atmospheric absorption template of 1998 February 19. Water-band correction proved to be critical for the detection of the CaT lines when the atmospheric conditions were most adverse.

Fig. 2 shows extractions of the nuclear 2 arcsec of the spectra of the galaxies. This corresponds to 844 to 2020 pc for the radio galaxies, and 98 pc for the normal elliptical galaxy.

3 LINE AND CONTINUUM MEASUREMENTS

3.1 CaT index

The CaT was detected in all of the objects, although in three cases (3C 285, 3C 382 and 4C 73.08) it was totally or partially affected by residuals left by the atmospheric-band corrections and the measurement of its strength was thus precluded. For the remaining cases, the strength was measured in the rest frame of the galaxies against a pseudo-continuum, following the definition of the CaT index of Díaz, Terlevich & Terlevich (1989). In Hydra A, 3C 285 and 3C 382, the red continuum band is seriously affected by residuals left from the atmospheric absorption removal. We defined two alternative continuum bands, $8575\,\text{Å} < \lambda < 8585\,\text{Å}$ and $8730\,\text{Å} < \lambda < 8740\,\text{Å}$, that substitute the red-most continuum

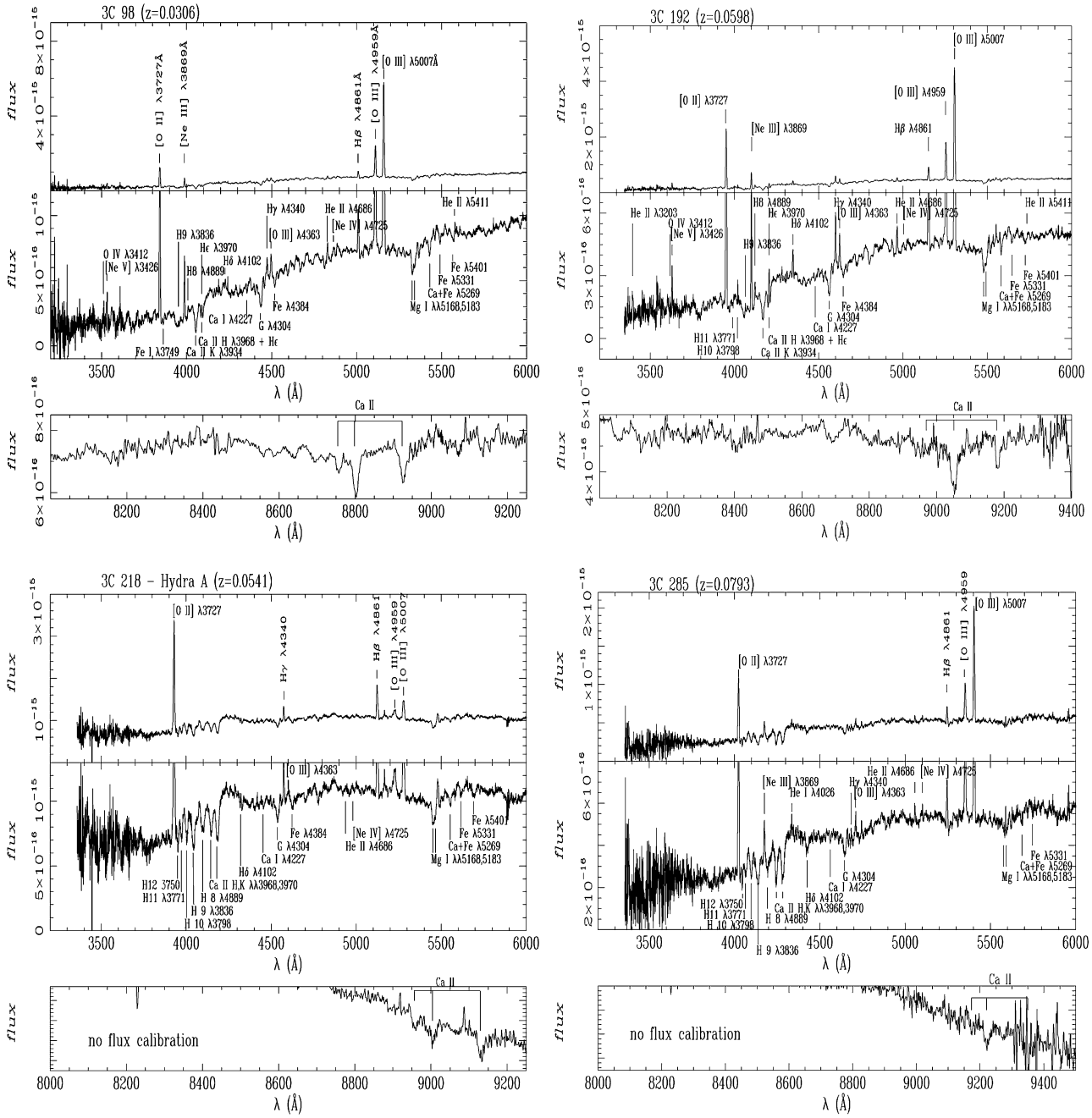

Figure 2. (a) Spectrum of 3C 98 in the observer's frame: top panel is scaled to show the emission lines detected in the blue-arm spectra; middle panel shows in greater detail the absorption lines in the same wavelength interval; bottom panel shows the CaT region detected in the red-arm spectra. (b) Spectrum of 3C 192. (c) Spectrum of Hydra A: the red-arm spectrum is not flux calibrated. (d) Spectrum of 3C 285: the red-arm spectrum is not flux calibrated. (e) Spectrum of 3C 382. (f) Spectrum of 4C 73.08. (g) Spectrum of DA 240. (h) Spectrum of NGC 4374.

window of the CaT index. We checked this new definition against the original one in the elliptical galaxy, which does not have residuals in its continuum bands, and the agreement between the two systems was good to within 5 per cent.

Velocity dispersions were measured by cross-correlating the galaxy spectra with the stellar spectra obtained with the same setup. The errors in the velocity dispersions calculated in this way were less than 10 per cent.

A high-velocity dispersion tends to decrease the measured values of indices based on equivalent width (EW) measurements. The CaT index has to be corrected from broadening of the absorption lines by the corresponding velocity dispersion. In order to calculate the correction we convolved stellar profiles with Gaussian functions of increasing width, and measured the CaT index in them. A good description of the correction found for our data is given by the functional form $\Delta\mathrm{EW(\AA)} = [\sigma(\mathrm{km\,s^{-1}}) - 100]/200$. The corrections were applied to the values measured in the galaxies, and converted into unbroadened indices.

The values of velocity dispersions (σ), uncorrected EW ($\mathrm{CaT_u}$) and corrected EW (CaT), are listed in Table 2.

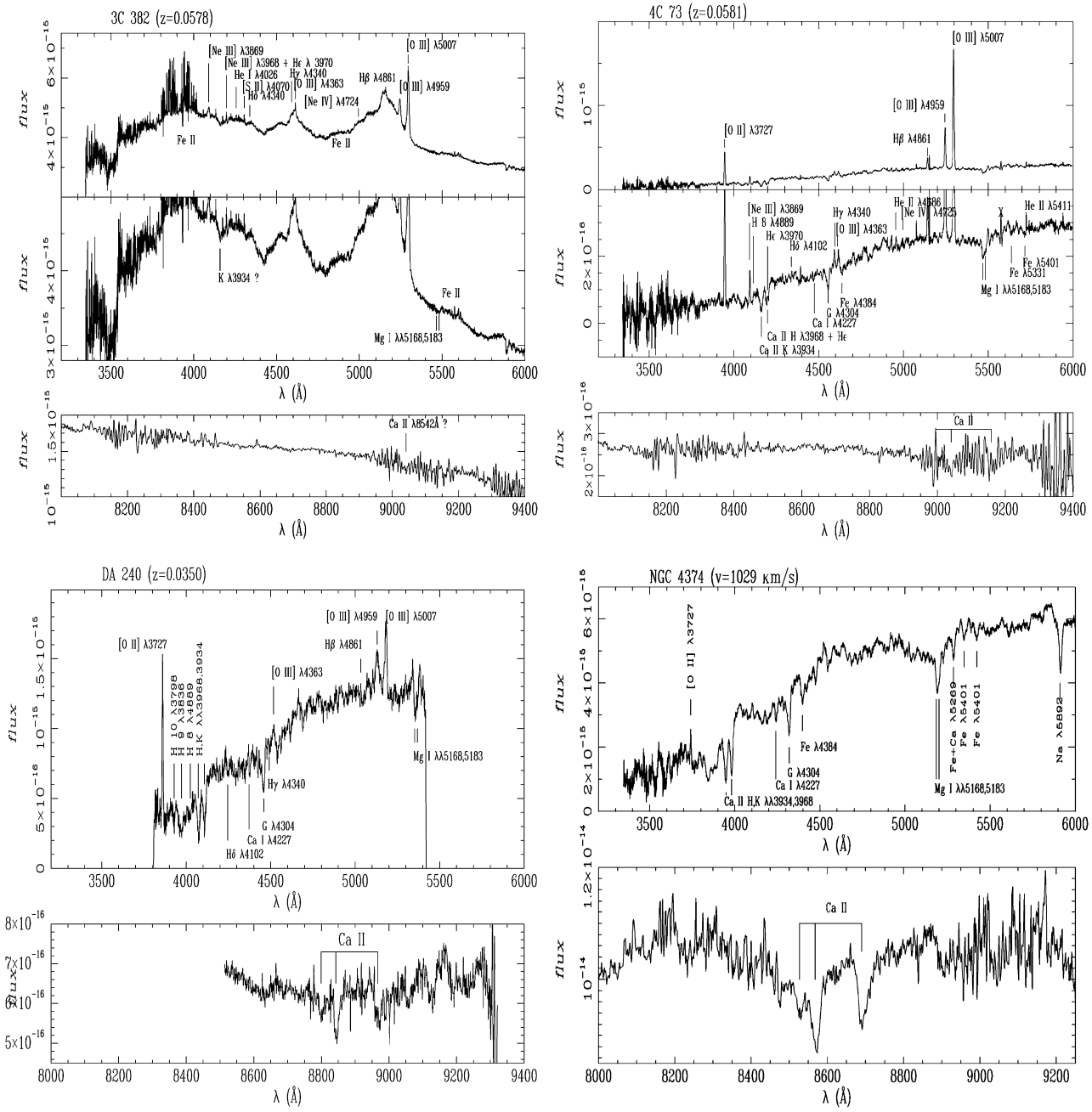

Figure 2. – *continued*

Table 2. Calcium triplet index and velocity dispersions.

object	σ km/s	CaT_u Å	CaT Å
3C 98	250	5.9	6.5
3C 192	241	5.4	6.0
Hydra A	292	6.1	7.0
3C 285	202	>2.4	–
4C 73.08	–	>5.2	–
DA 240	265	5.5	6.2
NGC 4374	361	5.3	6.8

3.2 λ4000-Å and Balmer break indices

Stellar populations can be dated through the measurement of the λ4000-Å or Balmer breaks. In intermediate-to-old populations, the discontinuity at λ4000 Å results from a combination of the accumulation of the Balmer lines towards the limit of the Balmer absorption continuum at λ3646 Å (the Balmer break) and the increase in stellar opacity caused by metal lines shortwards of λ4000 Å.

Table 3 lists the values of the λ4000-Å break index, Δ4000 Å, measured in the spectra of the six narrow-line radio galaxies and the elliptical galaxy in our sample. This excludes 3C 382, which has a spectrum dominated by a strong blue continuum and

Table 3. Break indices.

object	original spectra Δ4000 Å mag	bulge-subtracted spectra Δ4000 Å mag	D	λ_1 Å
3C 98	2.1			
3C 192	1.9			
Hydra A	1.4	1.2	0.26–0.28	3746–3752
3C 285	1.6	1.0	0.48–0.53	3740–3746
4C 73.08	2.2			
DA 240	2.2			
NGC 4374	2.3			

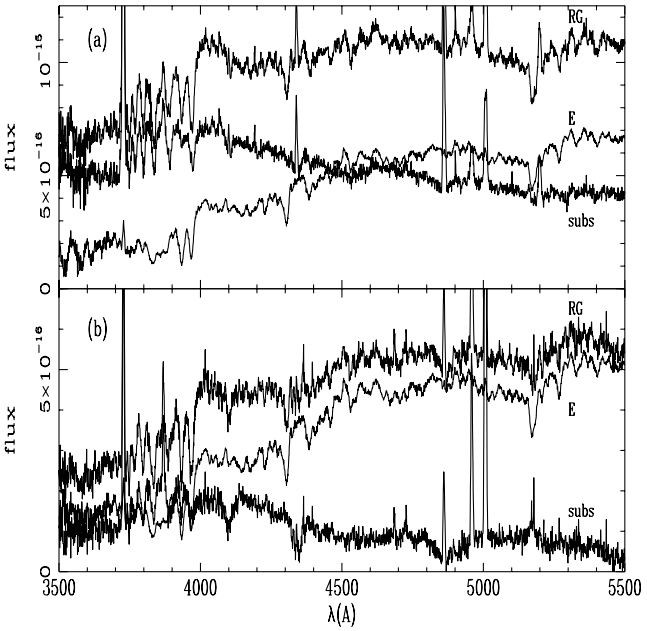

Figure 3. Bulge-subtraction for (a) Hydra A and (b) 3C 285. We show the original spectra of the radio galaxy (RG), the scaled template spectra of the bulge population (E), and the resulting bulge-subtracted spectra (subs).

broad-emission lines, and shows very weak stellar atmospheric features and no break. We adopted the definition given by Hamilton (1985), which quantifies the ratio of the average flux-level of two broad bands, one covering the break (3750–3950) and one bluewards of the break (4050–4250). Both bands contain strong metallic and Balmer absorption lines in the case of normal galaxies. In active galaxies, the measurement can be contaminated by emission of [Ne III]λ3869 Å, which in our case is weak. The contamination by high-order Balmer lines in emission is negligible. The net effect of emission contamination is to decrease the Balmer-break index. In the radio galaxies, we have estimated this effect by interpolating the continuum levels below the [Ne III] emission, and we estimate that the ratio can be affected by 6 per cent at worst, in the case of 3C 192, and by less than 3 per cent for the rest of the objects. Table 3 lists emission-devoid indices.

Hydra A and 3C 285 have spectra which are much bluer than those of normal elliptical galaxies. In order to quantify better the strength of the break and the ages of the populations derived, we have performed a bulge subtraction, using as a template the spectrum of NGC 4374, scaled to eliminate the G-band absorption of the radio galaxies. Since the velocity dispersion of the stars in NGC 4374 and in the radio galaxies are comparable inside the

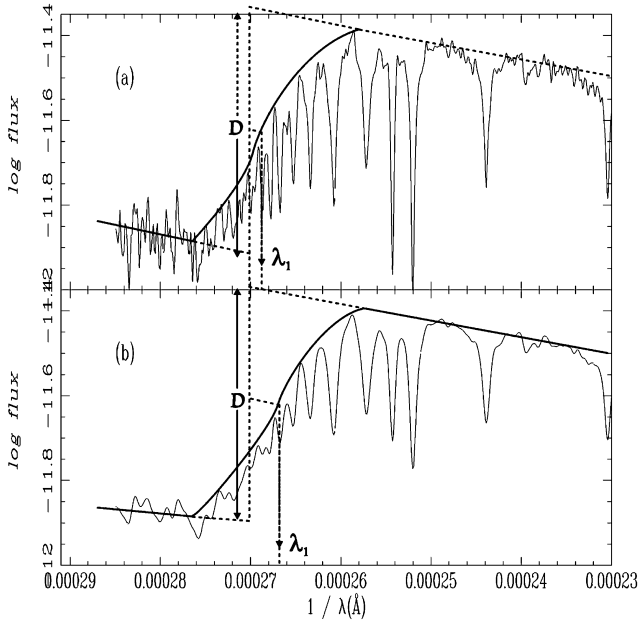

Figure 4. Balmer-break measurements of an A2I star: (a) original spectrum (b) spectrum convolved with a Gaussian filter to mimic the FWHM of the Balmer lines in the radio galaxies (≈12.5 Å). The solid lines trace the continua and pseudo-continua of the spectra, and the dashed lines depict the measurements of the corresponding $D\lambda_1$ values.

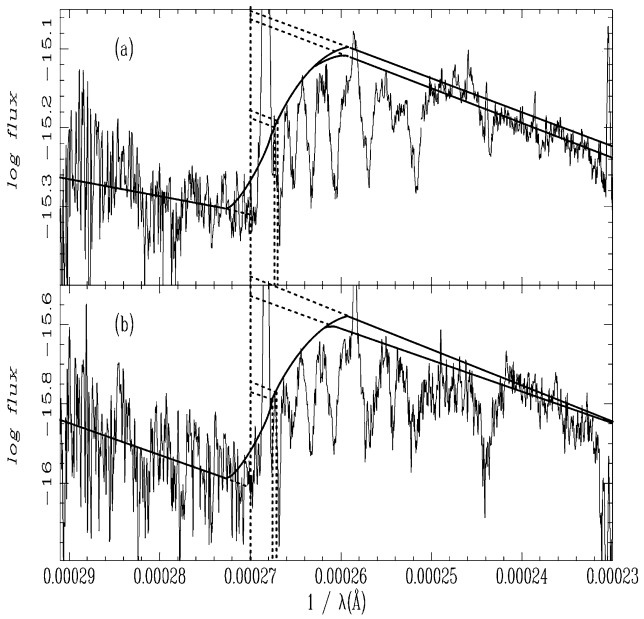

Figure 5. Balmer-break measurements of the bulge-subtracted spectra of (a) Hydra A and (b) 3C 285. The solid lines trace a wide range of allowed continua and pseudo-continua of the spectra, and the dashed lines their corresponding $D\lambda_1$ values.

spectral resolution of our data, no further corrections were needed. The G-band absorption is prominent in stars of spectral types later than F5 and it is especially strong in K-type stars. NGC 4374 is a normal elliptical galaxy, with a spectral shape which compares well with those of other normal ellipticals in the spectro-photometric atlas of galaxies of Kennicutt (1992). Thus, by removing a scaled template of NGC 4374, we are isolating the most massive stars ($M \gtrsim 1\,M_\odot$) in the composite stellar population

of the radio galaxies. Fig. 3 shows the bulge subtractions obtained for these two radio galaxies.

We measured the bulge-subtracted spectra Δ4000 Åand also the Balmer break index as defined by the classical $D\lambda_1$ method of stellar classification designed by Barbier (1955) and Chalonge (1956; see also Strömgren 1963). The index quantifies the Balmer discontinuity in terms of the logarithmic difference of the continuum levels (D) and the effective position of the break (λ_1). The method places a pseudo-continuum on top of the higher-order terms of the Balmer series in order to measure the effective position of the discontinuity. Fig. 4 shows the placement of continua, pseudo-continua and the measurements of D and λ_1 for an A2I star from the stellar library of Jacoby, Hunter & Christian (1984). The functional dependences on the effective temperature and gravity of the stars are sufficiently different for D and λ_1 to satisfy a two-dimensional classification.

The $D\lambda_1$ method could only be reliably applied in the cases of Hydra A and 3C 285. For the other radio galaxies, the bulge subtractions led to results that did not allow the identification of the absorption features and/or the break in an unambiguous way as a result of the resulting poor S/N. Fig. 5 shows the $D\lambda_1$ measurements performed on the bulge-subtracted spectra of Hydra A and 3C 285. We have shown different continuum levels to estimate the maximum range of acceptable parameters of the stellar populations that are involved.

Table 3 lists the λ4000-Å and Balmer-break indices measured in both the bulge-subtracted and the original spectra of the radio galaxies.

3.3 Lick indices

The presence of prominent Balmer absorption lines, from Hγ up to H12 λ3750 Å, is one of the most remarkable features of the blue spectra of two of the seven radio galaxies, while Hβ and Hα are filled up by conspicuous emission lines. A clear exception to the presence of the Balmer series in absorption is the broad-line radio galaxy 3C 382.

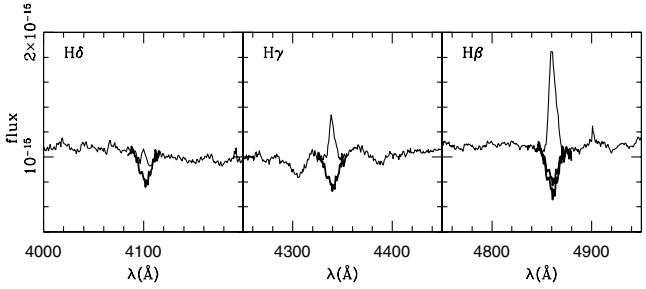

Figure 6. Estimated absorption profiles of low Balmer lines (thick line), compared with the actually observed profiles in Hydra A (thin line).

In order to estimate the Balmer strength, crucial to determining the age of any young stellar population involved, we use the EW of the H10 λ3798-Å line, which appears only weakly contaminated by emission in the radio galaxies. H10 is chosen as a compromise: it is an easily detectable Balmer line that shows both a minimum of emission contamination and clear wings to measure the adjacent continuum. The Balmer lines from Hβ to H9 λ3836 Å are contaminated by prominent emission, which in Case B recombination comes in decreasing emission ratios to Hβ of 1, 0.458, 0.251, 0.154, 0.102, and 0.0709 (Osterbrock 1989); H10 has an emission contamination of $0.0515 \times$ Hβ. At the same time, the absorption strengths are quite similar from Hβ to H10, although the EW(H10) is actually systematically smaller than EW(Hβ) in young to intermediate-age populations. González-Delgado, Heckman & Leitherer (2000) obtain, in their population synthesis models, ratios of EW(Hβ)/EW(H10) between 1.3 and 1.6 for bursts with ages 0 to 1 Gyr and constant or coeval star formation histories. Lines of order higher than 10 have decreasing emission contamination, but they also increasingly merge towards the Balmer continuum limit.

A caveat in the use of H10 as an age calibrator comes from the fact that this line might be contaminated by metallic lines in old populations. Although our measurements of H10 in NGC 4374 are around 1.5 Å, an inspection of the spectra of three elliptical galaxies (NGC 584, NC 720, NGC 821) observed in the same wavelegth range (but with lower S/N) and archived in the Isaac Newton Group data base, indicates that a wide range of EW(H10), from 2 to 4 Å, could characterize elliptical galaxies, while their Hβ indices are in the 1- to 2-Å regime. If confirmed by better data, these results could indicate that although the upper Balmer series is detected in elliptical galaxies, it could indeed be contaminated by the absorptions of other species. Clearly, more work needs to be done in the near-UV spectra of elliptical galaxies before conclusive evidence can be derived for the behaviour of EW(H10) in old stellar systems, and its contamination by metallic lines.

In all the radio galaxies observed in this work, the H10 profile is narrow and reproduces the shape of the wings of the lower-order Balmer absorption lines. Hydra A and 3C 285 clearly provide the best fittings. As an illustration, Fig. 6 shows the estimated absorption line profiles for the Hβ, Hγ and Hδ lines, assuming a constant ratio between their EWs and that of H10, and also a scaled (×1.4) H10 profile for the case of Hβ in Hydra A.

We also measured indices that are mostly sensitive to the metal content of the stellar populations involved. The Lick indices of Mg and Fe (e.g. Worthey et al. 1994) serve this purpose. In order to avoid the contribution of [O III]λ4959 Å to the continuum measurement for the molecular index Mg_2, we have displaced

Table 4. Lick indices.

object	Balmer Å	Mg b_u Å	Mg b Å	Fe5270$_u$ Å	Fe5270 Å	Fe5335$_u$ Å	Fe5335 Å	[MgFe] Å	Mg_{2u} mag	Mg_2 mag
3C 98	3.5	4.76	5.03	2.73	3.06	2.66	3.16	3.95	0.26	0.28
3C 192	>3.6	5.48	5.48	2.52	2.52	2.50	2.50	3.70	0.27	0.29
Hydra A	3.5	4.78	5.60	1.66	2.48	1.48	2.80	3.84	0.20	0.22
3C 285	4.4	3.37	3.51	1.67	1.85	1.50	1.76	2.52	0.18	0.20
4C 73.08	3.8	4.82	5.28	2.80	3.39	2.27	3.21	4.17	0.23	0.25
DA 240	4.5	4.01	4.28	–	–	–	–	–	–	–
NGC 4374	1.4	4.58	4.80	2.48	2.70	2.12	2.39	3.49	0.30	0.32

the lower continuum band of this index to 4895.125 Å $< \lambda <$ 4935.625 Å. This redefinition does not alter the value of the index in the elliptical galaxy, which shows no [O III] emission.

Table 4 compiles the EW of H10, and the metallic indices Mg b, Fe5270, Fe5335, [MgFe], Mg_2 of the Lick system, measured in the rest frame of the galaxies in our sample. The atomic indices are affected by broadening, like the CaT index, while Mg_2 is only affected by lamp contributions in the original IDS Lick system (Worthey et al. 1994; Longhetti et al. 1998). We have calculated broadening corrections as in Section 3.1 for the atomic lines, and adopted the corrections calculated by Longhetti et al. (1998) for the molecular lines. The uncorrected values of these indices are denoted with a subindex U in Table 4. The errors of the individual line and molecular indices were estimated adopting continua shifted from the best fit continua by $\pm 1\sigma$. This lead to average errors between 8 and 10 per cent for individual line and molecular indices, and ~6 per cent for [MgFe].

The agreement between our measurements of Lick indices and those carried out by other authors (González 1993; Davies et al. 1987; Trager et al. 2000a) on our galaxy in common, NGC 4374, is better than 10 per cent.

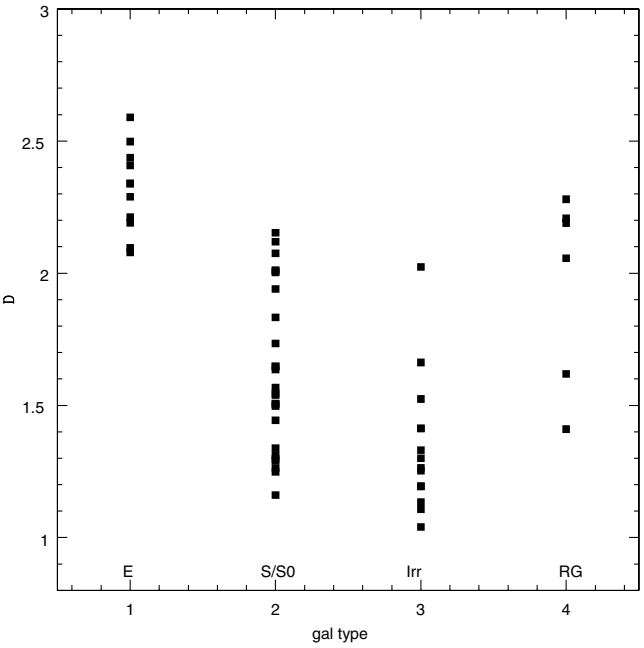

Figure 7. Δ4000-Å break measurements for the radio galaxies in our sample (RG) and for elliptical (E), spiral (S) and irregular (Irr) galaxies in the atlas of Kennicutt (1992).

4 DISCUSSION

4.1 Comparison with elliptical galaxies and population synthesis models

The analysis of the spectral energy distributions and colours of elliptical galaxies suffers from a well known age–metallicity degeneracy (Aaronson et al. 1978). However, this is broken down when the strengths of suitable stellar absorption lines are taken into account (e.g. Heckman 1980). The plane composed by the [Hβ] and [MgFe] indices, in this sense, can discriminate the ages and metallicities of stellar systems. It is on the basis of this plot that a large spread of ages in elliptical galaxies has been suggested (González 1993). Bressan, Chiosi & Tantalo (1996) claim, however, that when the UV emission and velocity dispersion of the galaxies are taken into account, the data are only compatible with basically old systems that have experienced different star formation histories (see also Trager et al. 2000a,b). A recent burst of star formation that involves only a tiny fraction of the whole elliptical mass in stars, would raise the [Hβ] index to values characteristic of single stellar populations which are 1–2 Gyr old (Bressan et al. 1996).

Most likely, the stellar populations of radio galaxies are also combinations of different generations. Direct support for this interpretation in the case of Hydra A comes from the fact that the stellar populations responsible for the strong Balmer lines are dynamically decoupled from those responsible for the metallic lines (Melnick, Gopal-Krishna & Terlevich 1997).

This interpretation is also consistent with the modest Δ4000 Å measurements we have obtained. Fig. 7 shows a comparison of the values found in radio galaxies, with those of normal elliptical, spiral and irregular galaxies, including starbursts, from the atlas of Kennicutt (1992). The radio galaxies 3C 98, 3C 192, 4C 73.08 and DA 240 have indices of the order of 1.9 to 2.3, which overlap with those of normal E galaxies, Δ4000 Å $= 2.08 \pm 0.23$. These values correspond to populations dominated by stars of ages 1 to 10 Gyr old, if one assumes the coeval population synthesis models of Longhetti et al. (1999). However, Hydra A and 3C 285 have indices in the range 1.4–1.6, typical of coeval populations which are 200 to 500 Myr old. Once the bulge population is subtracted, the Δ4000 Å indices of Hydra A and 3C 285 decrease to 1.2 and 1.0 respectively, which are typical of systems younger than about 60 Myr.

Hamilton (1985) measured the Δ4000-Å index in a sample of stars covering a wide range of spectral types and luminosity classes. He found a sequence of increasing Δ4000 Å from B0 to M5 stars, with values from 1–4 mag respectively. A comparison with the sequence he found leads us to conclude that the break in the bulge-subtracted spectrum of Hydra A is dominated by B- or earlier-type stars, while that of 3C 285 is dominated by A-type stars. The index Δ4000 Å does not clearly discriminate luminosity classes for stars with spectral types earlier than G0.

The equivalent width of the H10 absorption line in these two radio galaxies gives further support to the interpretation of the Balmer break as produced by a young stellar population. In Hydra A we find after bulge subtraction EW(H10) ≈ 3.9 Å, which, according to the synthesis models of González-Delgado et al. (2000) gives ages of 7–15 Myr for an instantaneous burst of star formation, and 40–60 Myr for a continuous star formation mode, in solar metallicity environments. In the case of 3C 285, EW(H10) ≈ 6 Å would imply an age older than about 25 Myr for a single-population burst of solar metallicity.

The metallic indices of normal elliptical galaxies range between the values $0.56 \lesssim \log[\mathrm{MgFe}] \lesssim 0.66$ (González 1993), which characterizes oversolar metallicities for ages greater than about 5 Gyr. This is also the typical range of our radio galaxies, although 3C 285 shows a clear departure with log[MgFe] ≈ 0.4. However, [MgFe] tends to be smaller for populations younger than a few Gyr and similar oversolar metallic content. Since 3C 285 has a clear burst of recent star formation, we conclude that its overall abundance is also most probably solar or oversolar.

4.2 The blue stellar content

A better estimate of the spectral type and luminosity class of the

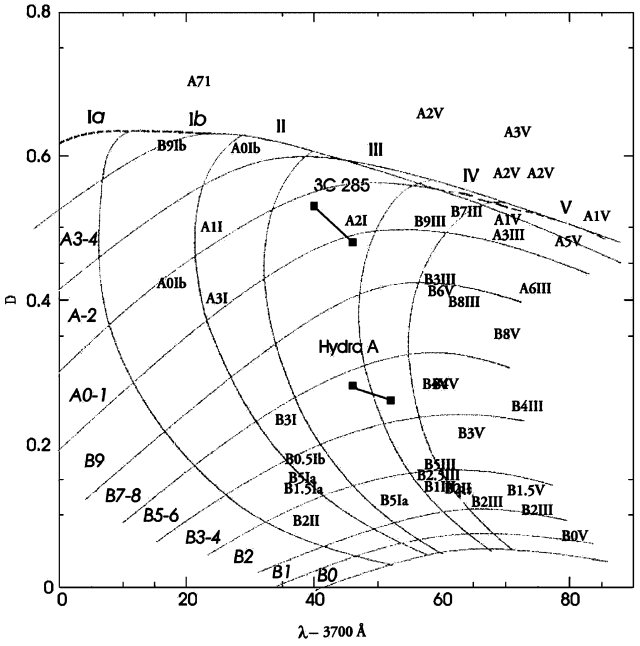

Figure 8. Barbier and Chalonge index plane. The location of the range of values for 3C 285 and Hydra A is indicated by solid squares and connecting lines. We have also plotted the indices measured in stars from the library of Jacoby et al. (1984), that have been broadened to mimic the width of the Balmer lines in the radio galaxies, represented by their corresponding spectral type and luminosity class (e.g. A2I). The grid of solid lines traces the original locus of unbroadened stars. The large symbols at the edges of the grid represent the correspondence with spectral classes and luminosity classes of the frame defined by the grid.

stars that dominate the break in Hydra A and 3C 285 comes from the two-dimensional classification of Barbier and Chalonge. In Fig. 8 the solid squares connected by lines represent the maximum range of possible $D\lambda_1$ values measured in these radio galaxies.

The Balmer-break index is sensitive to the positioning of the pseudo-continuum on top of the higher-order Balmer series lines, which in turn is sensitive to the merging of the wings of the lines, enhanced at large velocity dispersions. In order to assign spectral types and luminosity classes to the stars that dominate the break, therefore, it is not sufficient to compare the values we have obtained with those measured in stellar catalogues. The values measured for the radio galaxies can be corrected for their intrinsic velocity dispersions; we have chosen instead to recalibrate the index using template stars of different spectral types and luminosity classes convolved with Gaussian functions, until they reproduce the width of the Balmer lines observed in the radio galaxies (FWHM $\approx$ 12.5 Å). We used the B0 to A7 stars from the stellar library of Jacoby et al. (1984), which were observed with 4.5-Å resolution. The values of the $D\lambda_1$ indices measured in these broadened stars are represented in Fig. 8 by their respective classification. For comparison, we also plot the grid traced by the locus of unbroadened stars, as published by Strömgren (1963). The broadening of the lines shifts the original locus of supergiant stars from the $\lambda_1 \lesssim 3720$-Å range (Chalonge 1956) to the $3720 \lesssim \lambda_1 \lesssim 3740$-Å range, occupied by giant stars in the original (unbroadened) classification. Giant stars, in turn, shift to positions first occupied by dwarfs. Most dwarfs have Balmer line widths comparable to those of the radio galaxies, and thus their locus in the diagram is mostly unchanged.

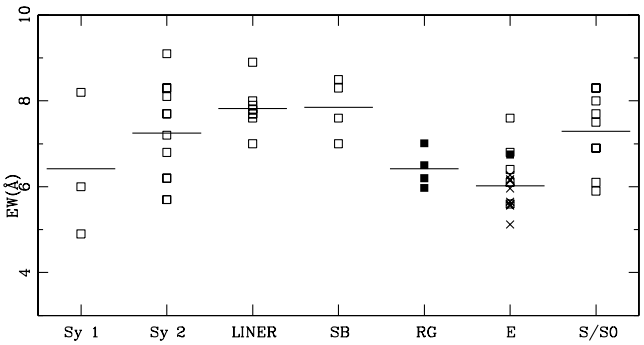

Figure 9. CaT index measured for the radio galaxies (RG), and compared with the values found in Seyfert 1 (Sy1), Seyfert 2 (Sy2), LINERs, starburst galaxies (SB), elliptical (E) and spiral and/or lenticular (S/S0) galaxies from the samples of Terlevich et al. (1990) and Gorgas et al. (priv. communication). Open squares: Terlevich et al. (1990). Crosses: Gorgas et al. (private communication). Filled squares: this work.

The value of the D index indicates that the recent burst in Hydra A is dominated by B3 to B5 stars, and the effective position of the Balmer break (λ_1) indicates that these are giant or supergiant stars, respectively. These stars have masses of 7 and 20 $M_\odot$ (Schmidt-Kaler 1982). From the stellar evolutionary tracks of massive stars with standard mass-loss rate at $Z_\odot$ or $2\,Z_\odot$ (Schaller et al. 1992; Schaerer et al. 1993; Meynet et al. 1994) we infer that these stars must have ages between 7 to 8 Myr (B3I) and 40 Myr (B5III). Note that the B4V stars in Fig. 8, near the location of Hydra A, cannot originate the break and at the same time follow the kinematics of the nucleus (see Section 5.3). Any dwarf star located in the stellar disc of Hydra A would show absorption lines that have been broadened beyond the 12.5 Å of FWHM we measure in this radio galaxy, and the position of the star would have been shifted further into larger values of λ_1.

The location in the $D - \lambda_1$ plane of 3C 285 indicates that the break is produced by A2I stars. These are 15-$M_\odot$ stars. Again, ages of 10 to 12 Myr are found for the last burst of star formation in this radio galaxy. The interpretation of the blue excess in terms of A type stars is further supported by the detection of the Ca II–H line in the bulge-subtracted spectrum.

4.3 The red stellar content

The CaT index in the radio galaxies has values between 6 and 7 Å. Díaz et al. (1989) find that at solar or oversolar metallicities, red supergiant stars have CaT indices ranging from 8.5–13 Å, red giant stars from 6–9 Å and dwarfs from 4.5–8.5 Å. The values we find are thus compatible with both giant or dwarf stars. However, we favour the interpretation of giant stars since the old bulge population will be dominated by red giants, as in the case of elliptical galaxies.

We have measured the CaT in a control sample of elliptical galaxies observed by J. Gorgas and collaborators (private communication) and have combined these measurements with those found by Terlevich et al (1990) in a sample of elliptical, lenticular, spiral, and active galaxies of different kinds. We find that the range of CaT in elliptical galaxies, 5–7.5 Å, comprises the range of values of the radio galaxies (see Fig. 9).

García-Vargas, Mollá & Bressan (1998) find, in their population synthesis models, values of the CaT between 6 and 7 Å for ages ranging from 100 Myr to 1 Gyr, and larger afterwards, assuming coeval star formation and solar or oversolar metallicity. A revised version of these models by Mollá & García-Vargas (2000), which

includes extended libraries of M-type stars, predicts (for ages between 2 and 20 Gyr) a constant value of 7 Å at solar metallicity, and 8.5 Å at 2 $Z_{\odot}$. These synthesis models are based on parametric fittings of the CaT strength in non-local thermodynamic equilibrium (NLTE) model atmospheres (Jørgensen, Carlsson & Johnson 1992) and in fittings of empirical values measured in stellar libraries (e.g. Díaz et al. 1989; Zhou 1991). The fits work well in the low-metallicity regime. However, at metallicities higher than solar, the relationship between metallicity and the CaT index shows a big scatter, and the linear fittings loose any predictive power (see fig. 4 of Díaz et al. 1989).

Red supergiant stars appear in coeval population synthesis models between 5 and 30 Myr, and create a maximum strength of the CaT index (CaT $\gtrsim$9 Å) around 6–16 Myr for $Z_{\odot}$ and 5–30 Myr for 2 $Z_{\odot}$ (García-Vargas et al. 1993, 1998; Mayya 1997). Strengths of CaT $\gtrsim$ 7 Å are characteristic of bursts with ages between 5 and 40 Myr. Leitherer et al. (1999) also find that the total strength of the population depends dramatically on the slope of the initial mass function (IMF) and star formation history. While a coeval burst with a complete Salpeter IMF yields values surpassing 7 Å between 6 and 12 Myr, the same IMF in a continuous star formation mode yields values of only 5.5 Å maximum. The CaT strength values for coeval star formation derived by Leitherer et al. (1999) differ substantially from those derived by García-Vargas and coworkers (1993, 1998) and by Mayya (1997), most probably as a result of a different calibration of the CaT index.

Mixed populations of young bursts which contain red supergiants, superposed on old populations, can also yield values of the CaT between 4 and 8 Å (García-Vargas et al. 1998). Since metal-rich giant stars have CaT values ranging from 6–9 Å, we regard our observations of the CaT index in radio galaxies as being compatible with ages 1–15 Gyr.

5 NOTES ON INDIVIDUAL OBJECTS

5.1 3C 98

3C 98 shows a double-lobe radio structure which spans 216 arcsec at 8.35 GHz, with a radio jet that crosses the northern lobe to hit a bright hotspot. There is little evidence of a southern jet, but a twin hotspot in the southern lobe is also present (Baum et al. 1988; Leahy et al. 1997; Hardcastle et al. 1998).

Broad-band imaging of the host of 3C 98 reveals a smooth and slightly elongated elliptical galaxy located in a sparse environment (Baum et al. 1988; Martel et al. 1999). Deeper images reveal a faint shell as a sign of a past disturbance (Smith & Heckman 1989). However, the rotation curves of 3C 98 show that the stellar kinematics has negligible rotation $<$25 km s^{-1} and no anomalies (Smith, Heckman & Illingworth 1990). Although the optical colours of 3C 98 are similar to those of normal elliptical galaxies (Zirbel 1996), one should note that the colours are modified by the high Galactic extiction towards the source, $A_V = 0.986$ (Schlegel et al. 1998). The Δ4000-Å and [MgFe] indices found in this radio galaxy are characteristic of old metal-rich populations.

An extended narrow-line region with a wealth of structure, and no particular orientation with respect to the radio axis, is also detected in direct narrow-band images (Baum et al. 1988). The narrow emission lines detected in the optical spectra correspond to highly ionized plasma (Baldwin, Phillips & Terlevich 1981; Saunders et al. 1989; Baum, Heckman & van Breugel 1992).

3C 98 has been detected in X-rays by the *Einstein* satellite at a flux level $f(0.5\text{–}3\,\mathrm{keV}) = 1 \times 10^{-13}\,\mathrm{erg\,cm^{-2}\,s^{-1}}$ or $L_X = 4.2 \times 10^{41}\,\mathrm{erg\,s^{-1}}$ (Fabbiano et al. 1984). The source detection was too weak to look for any extension to a point source.

5.2 3C 192

3C 192 has an 'X' symmetric double-lobe structure which extends 212 arcsec at 8.35 GHz, showing bright hotspots at the end of the lobes (Hogbom 1979; Baum et al. 1988; Hardcastle et al. 1998).

According to Sandage (1972), 3C 192 is a member of a small group of galaxies. Broad-band imaging reveals the host of 3C 192 to be a round elliptical galaxy with a companion of similar size 70 arcsec away, and no obvious signs of interaction (Baum et al. 1988; Baum & Heckman 1989). The stellar kinematics shows negligible rotation, $<$30 km s^{-1}, and no disturbances (Smith et al. 1990). The spectral shape of 3C 192 also shows a blue excess with respect to our template elliptical galaxy.

Extended narrow line-emission is detected, with structures which are cospatial with bridges and cocoons detected in radio emission (Baum et al. 1988). The narrow emission lines are highly ionized (Baldwin et al. 1981; Saunders et al. 1989; Baum et al. 1992).

The *Einstein* satellite detected 3C 192 in X-rays at a flux level $f(0.5\text{–}3\,\mathrm{keV}) = 1.1 \times 10^{-13}\,\mathrm{erg\,cm^{-2}\,s^{-1}}$, or $1.8 \times 10^{42}\,\mathrm{erg\,s^{-1}}$. The source is extended at a 97 per cent confidence level, $0.8^{+1.7}_{-0.3}$ arcmin, but a background object might be contaminating the map (Fabbiano et al. 1984).

5.3 3C 218 or Hydra A

3C 218 is one of the most luminous radio sources in the local ($z < 0.1$) Universe, only surpassed by Cygnus A. Although the radio luminosity of 3C 218 exceeds by an order of magnitude the characteristic FR I/FR II break luminosity, it has an edge-darkened FR I morphology (Ekers & Simkin 1983; Baum et al. 1988; Taylor et al. 1990). The total size of the radio structure extends for about 7 arcmin, such that the radio jets, which flare at 5 arcsec, are curved and display 'S' symetry.

3C 218 has been optically identified with the cD2 galaxy Hydra A (Simkin 1979), which dominates the poor cluster Abell 780. This, however, is an X-ray bright cluster with $L_{\mathrm{X}} \approx 2 \times 10^{44}\,\mathrm{erg\,s^{-1}}$ in the 0.5–4.5 keV range, as seen by the *Einstein* satellite (David et al. 1990). The total bolometric luminosity has been estimated to be $5 \times 10^{44}\,\mathrm{erg\,s^{-1}}$ from 0.4–2 keV *ROSAT* observations (Peres et al. 1998). The thermal model that best fits the data supports the existence of a cooling flow which is depositing mass in the central regions of the cluster at a rate of $264^{+81}_{-60}\,\mathrm{M_{\odot}\,yr^{-1}}$.

Hydra A has an associated type II cooling-flow nebula (Heckman et al. 1989), characterized by high Hα and X-ray luminosities, but relatively weak [N II] and [S II] and strong [O I] λ6300-Å emission lines, usually found in LINERs. The Hα extended narrow-line emission (Baum et al. 1988) actually fills the gap between the radio lobes.

The λ2200 Å, λ2700 Å, B-band, $B - V$ and, also, the $U - I$ continuum colours of the centre of Hydra A have been attributed to a $\sim$10 Myr burst of star formation involving 10^8 to $10^9\,\mathrm{M_{\odot}}$ (Hansen, Jørgensen & Nørgaard-Nielsen 1995; McNamara 1995). This is further supported by the detection of strong absorption lines of the Balmer series in the near-UV spectrum of the nucleus (Hansen et al. 1995; Melnick et al. 1997). We also find strong-absorption Balmer lines, which we identify as originating in blue supergiant or giant B stars. One of our best two matches in the $D\lambda_1$

classification we use in this work, B3I stars, also indicates ages 7 to 8 Myr.

Heckman et al. (1985) found that the stellar kinematics has negligible rotation ($13 \pm 18\,\mathrm{km\,s^{-1}}$), but their observations were limited to the λ4200–5700 Å region, and did not include the higher Balmer lines in absorption. On the other hand, Ekers & Simkin (1983) report very fast rotating stars in the central 20 kpc of the radio galaxy. A two-dimensional analysis of the blue spectrum shows a tilt of the Balmer absorption lines of $450 \pm 130\,\mathrm{km\,s^{-1}}$ in the central 3 arcsec, while the Ca II H and K lines do not show any displacement (Melnick et al. 1997). This tilt is further confirmed by our data. The conclusion derived by Melnick et al. (1997) is that the young stars have formed a disc which is rotating perpendicular to the position of the radio axis. The star formation disc has also been detected in *U*-band images McNamara 1995).

5.4 3C 285

The host galaxy of 3C 285 has been identified with the brightest member of a group of galaxies (Sandage 1972). Optical imaging of the galaxy reveals an elliptical main body and a distorted S-shaped envelope aligned with a companion galaxy ~40 arcsec to the north-west (Heckman et al. 1986). Narrow-band imaging shows that the S-shaped extension is the result of continuum-emitting structures (Heckman et al. 1986; Baum et al. 1988). The narrow emission lines are originated by photoionization with a high-ionization parameter (Saunders et al. 1989; Baum et al. 1992).

Sandage (1972) found that the $B - V$ colour of 3C 285 is much bluer than that of a normal elliptical galaxy. Our observations show that the blue light of the nucleus (inner 2 arcsec) is dominated by a burst which contains A2I stars, and thus has an age of 10–12 Myr.

Saslaw, Tyson & Crane (1978) identified a bright blue slightly resolved object halfway between the nucleus and the eastern radio lobe, which they denoted 3C 285/09.6. Optical spectra and imaging obtained by van Breugel & Dey (1993) showed that the knot is at the same redshift as the galaxy, and its *UBV* colours and 4000-Å break are consistent with a burst of 70 Myr, which they interpreted as being induced by the radio jet.

3C 285 is a classical double-lobed radio galaxy of 190 arcsec total extension at 4.86 GHz, with two hotspots and an eastern ridge showing curvature roughly along the line to the optical companion (Leahy & Williams 1984; Hardcastle et al. 1998).

The source has not been detected by the *Einstein* satellite in X-rays, at a flux level $f(0.5\text{–}3\,\mathrm{keV}) < 1.5 \times 10^{-13}\,\mathrm{erg\,cm^{-2}\,s^{-1}}$ or $L_X = 4.4 \times 10^{42}\,\mathrm{erg\,s^{-1}}$ (Fabbiano et al. 1984).

5.5 3C 382

3C 382 has a double-lobe structure, with a clear jet in the northern lobe that ends in a hotspot. A hotspot in the southern lobe is also detected, but a counterpart jet is not clear, although a trail of low fractional polarization is detected (Black et al. 1992). The total 3.85 GHz size between hotspots is 179 arcsec (Hardcastle et al. 1998).

Optically, the radiosource is identified with a disturbed elliptical galaxy dominated by a very bright and unresolved nucleus (Matthews, Morgan & Schmidt 1964; Martel et al. 1999), located in a moderately rich environment (Longair & Seldner 1979). The optical spectra show a strong continuum and prominent broad lines photoinized by a power-law type of spectrum (Saunders et al. 1989; Tadhunter, Fosbury & Quinn 1989). The stellar population of the host galaxy, as we show in our study, is barely detected in the nuclear regions.

The *Einstein* satellite detected 3C 382 in X-rays at a flux level $f(0.5\text{–}3\,\mathrm{keV}) = 1.3 \times 10^{-13}\,\mathrm{erg\,cm^{-2}\,s^{-1}}$, or $2 \times 10^{44}\,\mathrm{erg\,s^{-1}}$ (Fabbiano et al. 1984). The source is resolved in *ROSAT* HRI observations but its interpretation is debatable since the luminosity is too strong for a galaxy environment which is only moderately rich (Prieto 2000).

3C 382 is a variable source at X-ray (Dower et al. 1980; Barr & Giommi 1992), radio (Strom, Willis & Willis 1978), optical and UV frequencies (Puschell 1981; Tadhunter, Pérez & Fosbury 1986)

5.6 DA 240

This is a double-lobed giant radio galaxy of 34 arcmin angular size between hotspots and ongoing nuclear activity at 2.8 cm (Laing et al. 1983; Nilsson et al. 1993; Klein et al. 1994).

The amplitude of the angular cross-correlation of sources found in optical plates around the position of the radio source is weak, $A_{\mathrm{gg}} = 0.101 \pm 0.118$ (Prestage & Peacock 1988). Abell clusters at the same redshift have values $A_{\mathrm{gg}} \gtrsim 0.3$.

The optical spectra show weak Hβ and [Ne III] and [O III] narrow emission lines, compatible with a higly ionized medium which is obscured. The Δ4000-Å and [MgFe] indices found in this radio galaxy are characteristic of old metal-rich populations.

5.7 4C 73.08

4C 73.08 is a giant double-lobed radio-galaxy, with 13 arcmin angular size between hotspots (Mayer 1979; Nilsson et al. 1993).

The environment of the radio galaxy is also weak, with amplitude of the angular cross-correlation of optical galaxies around the radiosource of $A_{\mathrm{gg}} = 0.203$ (Prestage & Peacock 1988).

4C 73.08 shows a high-excitation spectrum typical of narrow-line radio galaxies. The colours of the radio galaxy and the Δ4000-Å and [MgFe] indices are comparable to those of our reference elliptical galaxy.

6 CONCLUSIONS

We have presented spectra of seven radio galaxies in the λ3350–6000 Å and λ7900–9400 Å range. All radio galaxies show either a clear detection or an indication of detection of the Ca II $\lambda\lambda$8494, 8542, 8662-Å triplet in absorption, and in six of them we detected Balmer absorption lines.

On the basis of the Δ4000-Å break measurements, we conclude that four of these radio galaxies contain populations which are typical of normal elliptical galaxies, two have populations younger than a few hundred Myr, and in one its stellar population cannot be characterized.

In the two cases with young bursts, Hydra A and 3C 285, we subtracted the bulge population using a normal elliptical galaxy as a template in order to better characterize the young burst. The λ4000-Å and Balmer-break index measurements indicate that the young population is dominated by blue giant and/or blue supergiant stars: B3I or B5III for Hydra A, and A2I for 3C 285. The derived age of the burst is beween 7 and 40 Myr for Hydra A, and 10 to 12 Myr for 3C 285.

The CaT strength, invoked to support the detection of young stellar populations in active galaxies, fails to provide a clear conclusion on the nature of the stars that dominate the red light in these radio galaxies. The CaT could either be a result of the red

giant stars that dominate old bulge populations, or of the red dwarfs of a young starburst ($t \lesssim 7$ Myr), or of the red giants and supergiants of a post-starburst ($t \gtrsim 30$ Myr), or of a combination of a bulge population and a recent burst of star formation. A mixed population is again favoured as the interpretation of the red spectra.

It is known that although the hosts of FR II sources look like ellipticals, few of them have true elliptical-galaxy properties: magnitudes, colours, and structural parameters show a wider dispersion than in normal ellipticals (Baum et al. 1988; Zirbel 1996). Most of the radio galaxies in our sample have reported structural disturbances in their optical morphologies, show signs of interactions, have close companions, belong to rich environments and/or have signatures of cooling flows. These are phenomena that facilitate carrying large quantities of gas to the centres of the galaxies and can power the AGN and/or provoke bursts of star formation.

Good quality data in the blue region of this sample is necessary in order to constrain the ages of the young populations involved, especially in the cases of 3C 98, 3C 192, DA 210, 3C 382 and 4C 73.08, where our bulge subtractions led to a poor signal-to-noise ratio and therefore unreliable results.

A detailed analysis of the ages of the last burst of star formation will establish the relative chronology of the onset of the radio and starburst activity in these galaxies, and shed new light on the relationships between jets, AGN and star formation.

ACKNOWLEDGMENTS

This work has been supported in part by the 'Formation and Evolution of Galaxies' Network set up by the European Commission under contract ERB FMRX-CT96-086 of its TMR programme. We thank PATT for awarding observing time. IA, ET and RJT also thank the Guillermo Haro Programme for Advanced Astrophysics of Instituto Nacional de Astrofísica, Óptica Electrónica for the oportunity it gave us to meet and make progress on the project during the 1998 workshop 'The Formation and Evolution of Galaxies'. GC acknowledges a Particle Physics and Astronomy Research Council Postdoctoral Research Fellowship, and ET an IBERDROLA Visiting Professorship to the Universidad Autónoma de Madrid. We thank J. Gorgas for providing the CaT spectra of the sample of comparison elliptical galaxies prior to publication, M. García-Vargas for suggestions on how to improve the fringing removal, and an anonymous referee for crucial comments on the relevance of Balmer indices in old populations.

The William Herschel Telescope is operated on the island of La Palma by the Isaac Newton Group in the Spanish Observatorio del Roque de los Muchachos of the Instituto de Astrofísica de Canarias.

REFERENCES

Aaronson M., Cohen J. G., Mould J. R., Malkan M., 1978, ApJ, 223, 824
Baldwin J. A., Phillips M. M., Terlevich R. J., 1981, PASP, 93, 5
Barbier D., 1955, Contrib. Inst. d'Astrophysique Paris (A), 178, 8
Barr P., Giommi P., 1992, MNRAS, 255, 495
Baum S. A., Heckman T. M., 1989, ApJ, 336, 681
Baum S. A., Heckman T. M., Bridle A. H., van Breugel W. J. M., Miley G. K. M., 1988, ApJS, 68, 643
Baum S., Heckman T. M., van Breugel W., 1992, ApJ, 389, 208
Black A. R. S., Baum S. A., Leahy J. P., Perley R. A., Riley J. M., Scheuer P. A. G., 1992, MNRAS, 256, 186
Bressan A., Chiosi C., Tantalo R., 1996, A&A, 311, 425
van Breugel W. J. M., Dey A., 1993, ApJ, 414, 563
Chalonge D., 1956, Ann. Astrophys., 19, 258
Cid Fernandes R., Terlevich R., 1995, MNRAS, 272, 423
Cid Fernandes R., Rodrigues-Lacerda R., Schmitt H.-R., Storchi-Bergmann T., 1999, in van der Hucht K. A., Koenigsberger G., Eenens P. R. J., eds, IAU Symp. 193, Wolf-Rayet Phenomena in Massive Stars and Starburst Galaxies. Astron. Soc. Pac., San Francisco, p. 590
Colina L., Garcia Vargas M. L., González Delgado R. M., Mas-Hesse J. M., Perez E., Alberdi A., Krabbe A., 1997, ApJ, 488, 71
David L. P., Arnaud K. A., Forman W., Jones C., 1990, ApJ, 356, 32
Davies R. L., Burstein D., Dressler A., Faber S. M., Lynden-Bell D., Terlevich R. J., Wegner G., 1987, ApJS, 64, 58
Díaz A. I., Terlevich E., Terlevich R. J., 1989, MNRAS, 239, 327
Dower R. G., Griffiths R. E., Bradt H. V., Doxsey R. E., Johnson M. D., 1980, ApJ, 235, 355
Ekers R. D., Simkin S. M., 1983, ApJ, 265, 85
Fabbiano G., Trinchieri G., Elvis M., Miller L., Longair M., 1984, ApJ, 277, 115
Fanaroff B., Riley J., 1974, MNRAS, 167, 31
García-Vargas M. L., Díaz A. I., Terlevich E., Terlevich R. J., 1993, Ap&SS, 205, 85
García-Vargas M. L., Mollá M., Bressan S., 1998, A&AS, 130, 513
González J., 1993, PhD thesis, Univ. Santa Cruz
González Delgado R. M., Heckman T., Leitherer C., Meurer G., Krolik J., Wilson A. S., Kinney A., 1998, ApJ, 505, 174
González Delgado R. M., Heckman T. M., Leitherer C., 2000, ApJ, 546, 845
Hamilton D., 1985, ApJ, 297, 371
Hansen L., Jørgensen H. E., Nørgaard-Nielsen H. U., 1995, A&A, 297, 13
Hardcastle M., Alexander P., Pooley G. G., Riley J. M., 1998, MNRAS, 296, 445
Heckman T. M., 1980, A&A, 87, 142
Heckman T. M., Illingworth G. D., Miley G. K., van Breugel W. J. M., 1985, ApJ, 299, 41
Heckman T. M., Smith E. P., Baum S. A., van Breugel W. J. M., Miley G. K., Illingworth G. D., Bothun G. D., Balick B., 1986, ApJ, 311, 526
Heckman T. M., Baum S. A., van Breugel W. J. M., McCarthy P. A., 1989, ApJ, 338, 48
Heckman T. M. et al., 1995, ApJ, 452, 549
Heckman T. M., González-Delgado R., Leitherer C., Meurer G. R., Krolik J., Wilson A. S., Koratkar A., Kinney A., 1997, ApJ, 482, 114
Hogbom J. A., 1979, ApJS, 36, 173
Jacoby G. H., Hunter D. A., Christian C. A., 1984, ApJS, 56, 257
Jiménez-Benito L., Díaz A. I., Terlevich R. J., Terlevich E., 2000, MNRAS, 317, 907
Jørgenssen U. G., Carlsson M., Johnson H. R., 1992, A&A, 254, 258
Kennicutt R., 1992, ApJS, 79, 255
Klein U., Mack K.-H., Strom R., Wielebinski R., Achatz U., 1994, A&A, 283, 744
Kunth D., Contini T., 1999, in van der Hucht K. A., Koenigsberger G., Eenens P. R. J., eds, IAU Symp. 193, Wolf-Rayet Phenomena in Massive Stars and Starburst Galaxies. Astron. Soc. Pac., San Francisco, p. 725
Laing R. A., Riley J. M., Longair M. S., 1983, MNRAS, 204, 151
Leahy J. P., Williams A. G., 1984, MNRAS, 210, 929
Leahy J. P., Bridle A. H., Strom R. G., 1996, An Atlas of DRAGNs. http@//www.jb.man.ac.uk/atlas/
Leahy J. P., Black A. R. S., Dennett-Thorpe J., Hardcastle M. J., Komissarov S., Perley R. A., Riley J. M., Scherer P. A. G., 1997, MNRAS, 291, 20
Leitherer C. et al., 1999, ApJS, 123, 3
Longair M. S., Seldner R., 1979, MNRAS, 189, 433
Longhetti M., Bressan A., Chiosi C., Rampazzo R., 1998, A&AS, 130, 251
Longhetti M., Bressan A., Chiosi C., Rampazzo R., 1999, A&A, 345, 419
Maoz D., Filippenko A. V., Ho L. C., Rix H.-W., Bahcall J. N., Schneider D. P., Macchetto F. D., 1995, ApJ, 440, 91

Maoz D., Koratkar A., Shields J. C., Ho L. C., Filippenko A. V., Stenberg A., 1998, AJ, 116, 55
Martel A. R. et al., 1999, ApJS, 122, 81
Matthews T. A., Morgan W. M., Schmidt M., 1964, ApJ, 272, 400
Mayer C. J., 1979, MNRAS, 186, 99
Mayya D., 1997, ApJ, 482, L149
Melnick J., Gopal-Krishna, Terlevich R. J., 1997, A&A, 318, 337
Meynet G., Maeder A., Schaller G., Schaerer D., 1994, A&AS, 103, 97
Miller J. S., Goodrich R. W., 1990, ApJ, 355, 456
Mollá M., García-Vargas M. L., 2000, A&A, 359, 18
Nilsson K., Valtonen M. J., Kotilainen J., Jaakkola T., 1993, ApJ, 413, 453
Oliva E., Origlia L., Kotilainen J. K. J., Moorwood A. F. M., 1995, A&A, 301, 55
Osterbrook D. E., 1989, Astrophysics of Gaseous Nebulae and Active Galactic Nuclei. University Science Books, Mill Valley CA, also Oxford Univ. Press, Oxford
Peres C. B., Fabian A. C., Edge A. C., Allen S. W., Johnstone R. M., White D. A., 1998, MNRAS, 298, 416
Perry J., Dyson J. E., 1985, MNRAS, 213, 665
Peterson B. M., 1992, in Filippenko A. V., ed., ASP Conf. Ser. 31, Relationships between AGN and SB galaxies. Astron. Soc. Pac., San Francisco, p. 29
Prestage R. M., Peacock J. A., 1988, MNRAS, 230, 131
Prieto M. A., 2000, MNRAS, 316, 442
Puschell J. J., 1981, AJ, 86, 16
Rawlings S., Saunders R., 1991, Nat, 349, 138
Sandage A., 1972, ApJ, 178, 25
Saslaw W. C., Tyson J. A., Crane P., 1978, ApJ, 222, 335
Saunders R., Baldwin J. E., Rawlings S., Warner P. J., Miller L., 1989, MNRAS, 238, 777
Schaerer D., Meynet G., Maeder A., Schaller G., 1993, A&AS, 98, 523
Schaller G., Schaerer D., Meynet G., Maeder A., 1992, A&AS, 96, 269
Schlegel D. J., Finkbeiner D. P., Davis M., 1998, ApJ, 500, 525
Schmidt-Kaler T., 1982, in Schaifers K., Voigt H. H., eds, Landolt-Börnstein, New Series, Group VI, vol. 2b. Springer-Verlag, Berlin
Scoville N., Norman C., 1988, ApJ, 332, 163
Simkin S. M., 1979, ApJ, 234, 56
Smith E. P., Heckman T. M., 1989, ApJ, 341, 658
Smith E. P., Heckman T. M., Illingworth G. D., 1990, ApJ, 356, 399
Strom R. G., Willis A. G., Willis A. S., 1978, A&A, 68, 367
Strömgren B., Strand K. A., 1963, 'Basic Astronomical Data Stars', Stars and Stellar Systems, vol. 3. Univ. Chicago Press, Chicago, p. 123
Tadhunter C. N., Pérez E., Fosbury R. A. E., 1986, MNRAS, 219, 555
Tadhunter C. N., Fosbury R. A. E., Quinn P. J., 1989, MNRAS, 240, 225
Taylor G. B., Perley R. A., Inoue M., Kato T., Tabara H., Aizu K., 1990, ApJ, 360, 41
Terlevich E., Díaz A. I., Terlevich R., 1990, MNRAS, 242, 285
Terlevich R., Melnick J., 1985, MNRAS, 213, 841
Terlevich R., Tenorio-Tagle G., Franco J., Melnick J., 1992, MNRAS, 255, 713
Trager S. C., Faber S. M., Worthey G., González J. J., 2000a, AJ, 119, 1645
Trager S. C., Faber S. M., Worthey G., González J. J., 2000b, AJ, 120, 165
Tran H. D., Miller J. S., Kay L. E., 1992, ApJ, 397, 452
de Vaucouleurs G., de Vaucouleurs A., Corwin H. G., Buta R. J., Paturel G., Fouque P., 1991, Third Reference Catalogue of Bright Galaxies. Springer-Verlag, Berlin
Worthey G., Faber S. M., González J. J., Burstein D., 1994, ApJS, 94, 687
Zhou X., 1991, A&A, 248, 367
Zirbel E. L., 1996, ApJ, 473, 713

This paper has been typeset from a TEX/LATEX file prepared by the author.